https://doi.org/10.5194/egusphere-2024-1390
Preprint. Discussion started: 11 July 2024

Technical note: Quantified organic aerosol subsaturated hygroscopicity by a simple optical scatter monitor system through field measurements

Jie Zhang[1], Tianyu Zhu[1,2], Alexandra Catena[1], Yaowei Li[3], Margaret J. Schwab[1], Pengfei Liu[4], Akua A. Asa-Awuku[5], James Schwab[1]

[1]Atmospheric Sciences Research Center, University at Albany, State University of New York, Albany, NY, 12226, United States
[2]Department of Atmospheric and Environmental Sciences, University at Albany, State University of New York, Albany, NY, 12226, United States
[3]School of Engineering and Applied Sciences, Harvard University, Cambridge, MA, 02138, United States
[4]School of Earth and Atmospheric Sciences, Georgia Institute of Technology, Atlanta, GA, 30332, United States
[5]Department of Chemical and Biomolecular Engineering, A. James Clark School of Engineering, University of Maryland, College Park, MD, 20742, United States

Correspondence to: Jie Zhang (jzhang35@albany.edu)

Abstract. The hygroscopicity of organic aerosol (κ_{OA}) plays a crucial role in cloud droplet activation and aerosol-radiation interactions. This study investigated the viability of an optical scatter monitor system, featuring two nephelometric monitors (pDR-1500), to determine κ_{OA}, after knowing the aerosol chemical composition. This system was operated during a mobile lab deployment on Long Island in the summer of 2023, which was executed to coordinate with the Atmospheric Emissions and Reactions Observed from Megacities to Marine Areas (AEROMMA) field campaign. The derived κ_{OA} under subsaturated high humidity conditions (RH between 85% and 95%) were categorized based on different aerosol sources, including wildfire aerosol, urban aerosol, and aerosol from rural conditions. The κ_{OA} and the OA O:C ratio exhibited linear positive relationships for the urban aerosol and the aerosol from rural conditions, with a much higher slope (0.50 vs. 0.24) for the latter. However, there was no clear relationship between κ_{OA} and the OA O/C ratio observed during each period affected by wildfire plumes. The system proposed here could be widely applied alongside the current aerosol component measurement systems, providing valuable insights into the large-scale spatial and temporal variations of OA hygroscopicity.

1 Introduction

Aerosol hygroscopic growth under subsaturated high humidity remains one of the most important research topics in aerosol hygroscopicity (Liu et al., 2018; Wang et al., 2022). This phenomenon can directly determine aerosol liquid water (ALW), which can in turn impact the chemical composition and optical properties of aerosols through aqueous reactions and enhanced light scattering under ambient conditions (Ervens et al., 2011). Additionally, it plays a crucial role in the aerosol's ability to form cloud condensation nuclei (CCN), which can significantly influence cloud formation, related indirect radiative forcing, and in-cloud aqueous chemistry (Seinfeld et al., 2016; Pöhlker et al., 2023). The hygroscopicity parameter under subsaturated conditions (κsub, hereafter "κ" for simplicity) is commonly used to represent the aerosol hygroscopic activity/growth (Petters et al., 2007). κ can be further divided into the inorganic aerosol hygroscopicity (κ_{IOA}), which can be inferred from aerosol inorganic compound mass concentration, temperature and RH (Lance et al., 2013; Cerully et al., 2015), and organic aerosol hygroscopicity (κ_{OA}), which is still poorly characterized due to limited knowledge of organic species sources and formation pathways (Jimenez et al., 2009; Shrivastava et al., 2017).

The most common method for deriving κ_{OA} involves (1) estimating κ from the hygroscopic growth factor (HGF) measured by the humidified tandem differential mobility analyzers (HTDMA) (Petters et al., 2007; Wu et al., 2013) and (2) calculating κ_{IOA} from the inorganic aerosol mass concentration measured by the co-located Aerosol Mass Spectrometer (AMS) (Zhang et al., 2007) or Aerosol Chemical Speciation Monitor (ACSM) (Ng et al., 2011) through the thermodynamic equilibrium model (Fountoukis et al., 2007). However, the combination of these two complicated and expensive instruments (HTDMA and AMS/ACSM) significantly limited their widespread applications for κ_{OA} estimation on both spatial and temporal scales. Numerous studies have reported positive correlations between κ_{OA} and the aerosol oxidation state (e.g., O:C ratio) (Chang et al., 2010; Massoli et al., 2010; Cappa et al., 2011; Lambe et al., 2011; Kuwata et al., 2013; Richards et al., 2013) and have suggested a potential method to estimate κ_{OA} based on the measured O:C ratio. However, significant discrepancies exist in these relationships, underscoring the critical need for developing a simplified method or system to obtain κOA with the potential for long-term and widespread application, to explore these relationships.

Zhang et al. (2020) demonstrated the quantitative relationship between the response of the Thermo pDR-1500 (hereafter referred to as "pDR," a type of nephelometric/optical scatter monitor) under subsaturated high relative humidity (RH) conditions and aerosol liquid water (ALW). Building on this, this study extends the application of the optical scatter instrument system introduced by Zhang et al. (2020) to estimate ALW based on the 2023 summer field measurements. ALW is further used to estimate the ALW_{OA} based on the aerosol chemical composition measured by an AMS and subsequently used to estimate κ_{OA}. The derived κ_{OA} was categorized based on the different aerosol sources, and its relationship with the measured organic aerosol O/C ratio was discussed. Additionally, a comparison with previous studies is conducted to validate the feasibility of this system.

2 Section (as Heading 1)

2.1 Field campaigns

The field measurements were conducted from June 21, 2023 to Sep. 07, 2023 in Long Island, NY, utilizing our Atmospheric Sciences Research Center (hereafter "ASRC") mobile lab. The data collection involved a combination of on-road measurements for some special case days and off-road measurements while parked beside the Flax Pond Marine Laboratory, Stony Brook University. The ASRC mobile lab is a well-equipped platform featuring an aerosol HR-ToF-AMS for aerosol chemical component mass concentration, two pDRs (one for dry aerosol and one for wet aerosol, as described in

Fig. 1), a condensation particle counter (CPC) for aerosol number concentration, several gas monitors (i.e., O_3, NO_2, CO_2, HCHO, CH_4, etc.) and an Airmar meteorological monitor. Further details about the ASRC mobile lab can be found in Zhang et al. (2018). In this study, the measurements from AMS and the two pDRs were used with a time-averaging period of one hour.

The on-road measurement field campaigns were executed as the "2023 Mobile Laboratory Measurements of the Atmospheric Chemical Evolution in Urban Outflow Plumes and their Interplay with Coastal Meteorology over Long Island" project. This project aims to study the ozone/aerosol chemistry dynamics in the urban plume in the lowest layer under the influence of the coastal meteorology over Long Island, urban heatwave, and other extreme events. It is also designed to fully coordinate with and complement other comprehensive field campaigns - Atmospheric Emissions and Reactions Observed from Megacities to Marine Areas (AEROMMA), the New York City region for the Coastal Urban Plume Dynamics Study (CUPiDS), and the Synergistic TEMPO Air Quality Science (STAQS), during 2023 summer over NYC and its downwind regions including Long Island. More detailed information about the above campaigns can be found at https://csl.noaa.gov/projects/aeromma.

Throughout the measurement period, several periods were significantly influenced by urban plumes from the eastern coastal urban regions, rural plumes from the remote region, or by wildfire plumes transported from western Canada. The days with similar aerosol sources will be classified into one group with a total of three different groups identified in this study. All these provided a unique opportunity to explore the variation of κ_{OA} of each group and its relationship with the measured O:C ratio of organic aerosol from each source.

2.2 System setup

A schematic of the setup for κ_{OA} estimation used in the ASRC mobile lab is depicted in Fig. 1, comprising two pDRs, one Aerodyne high-resolution time-of-flight aerosol mass spectrometer (HR-ToF-AMS, hereafter "AMS"), and one TSI silica dryer (Diffusion Dryer 3062). During the measurements, one pDR was installed downstream of the silica dryer for the dry aerosol mass concentration (hereafter "pDR_{dry}"), and one pDR was directly connected to the ambient air under ambient RH conditions for the wet aerosol mass concentration (hereafter "pDR_{wet}"). The AMS was used to measure the aerosol chemical component mass concentration (including organic, sulfate, nitrate, ammonia, and chlorine), the O:C ratio, and also used as the reference aerosol mass concentration instrument to calibrate the pDR measurements. Meanwhile, data collected under the lowest relative humidity conditions reported by pDR_{wet} (RH < 45%) were utilized to generate a self-correlation scatterplot between the two pDRs (Fig. S1), which was applied to all data from pDRwet before all further data analysis.

In the mobile lab setup, ambient air was drawn at a flow rate of around 56 liters per minute into a stainless steel tube with a 2.5 cm diameter, equipped with a PM cyclone (URG-2000-30EC) designed to filter particles larger than 2 μm. The TSI silica dryer and pDRwet were linked to the sampling duct of the stainless steel tube via black conductive tubing with an internal diameter of 4.5mm. The tubing lengths were approximately 0.3 meters for the TSI silica dryer and 1 meter for the pDRwet. After The TSI silica dryer (roughly 0.5m long), the pDR_{dry} and AMS were connected to the dryer output through a

0.2m black tubing parallelly. Varied lengths of black tubing were employed to maintain a roughly consistent total airflow path to the pDR_{dry}, pDR_{wet}, and AMS. The estimated particle loss from the van inlet to each instrument was less than 1% (https://www.mpic.de/4230607/particle-loss-calculator-plc).

The selection of pDR is based on its capability to report both the temperature and RH of the aerosol flow, along with the aerosol mass concentration. The pDR is a type of nephelometric monitor that utilizes an LED light source with a wavelength of 880nm. It measures particle scattering within a forward scattering angle range of 60 to 80 degrees. The device converts the intensity of the scattered light it detects into mass concentration values based on the factory calibration, which was aligned with a gravimetric standard Arizona Road Dust (Zhang et al., 2018). The calibration factor for the pDR, defined as the ratio of the aerosol mass concentration reported by the pDR to that of a reference instrument, was shown to be directly proportional to the relative scattering intensity calculated using Mie theory (Zhang et al., 2018). Furthermore, this calibration factor was proven to be little affected by relative humidity (RH) variations within the range of 65 to 95%, maintaining an accuracy with an error margin of less than 5%. In this way, the aerosol mass concentration reported by pDR_{wet} (hereafter "M_{pDRwet}", units: µg m^{-3}) can be calibrated based on the calibration factor derived from the aerosol mass concentration measured from pDR_{dry} (hereafter "M_{pDRdry}", units: µg m^{-3}) and from the reference instrument (AMS in this study, M_{AMS} for the measured mass concentration, units: µg m^{-3}). Any increase in the mass concentration measured by the calibrated pDRwet compared to that of the calibrated pDRdry can be attributed solely to the presence of ALW (Zhang et al., 2020).

Both pDR devices were fitted with a "Blue Cyclone" and had their flow rates set to 1.5 LPM, achieving an aerosol diameter 50% cut point of 2.5 µm. This cut point was chosen to be 2.5 µm, instead of the 1µm (upper size limit of the AMS), to accommodate the enlargement of aerosols under high RH conditions when using the pDR_{wet}. However, the difference in the size range between the pDR devices and the AMS introduced a level of uncertainty to the proposed method, which will be addressed in the following discussion. It is also important to note that the temperature and RH obtained from pDR_{wet} were measured inside of pDR_{wet} and could be affected by the inside temperature of the mobile lab and the calculated ALW may not accurately represent the real ALW of the ambient aerosol.

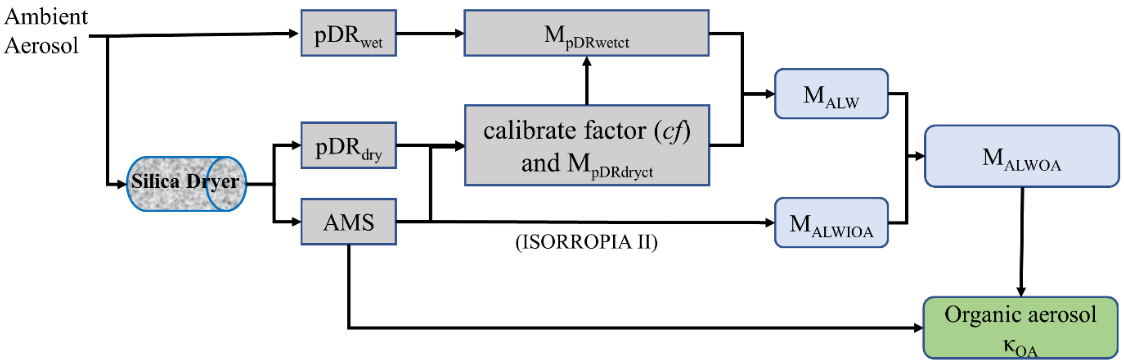

Figure 1. Schematic of the experimental setup for the organic aerosol hygroscopicity (κ_{OA}) estimation.

As shown in Fig.1 and described more fully in our previous study (Zhang et al., 2020), mass of ALW (hereafter "MALW", units: µg m-3) can be obtained from the subtraction of the calibrated aerosol mass concentration from pDR_{dry} (hereafter "$M_{pDRdryc}$") from the calibrated aerosol mass concentration pDR_{wet} (hereafter "$M_{pDRwetc}$"), as shown in Eq.(1):

$$M_{ALW} = M_{PDRwetc} - M_{PDRdryc} \quad (1)$$

Here $M_{pDRdryc}$ was set equal to the aerosol mass concentration measured by AMS, and a calibration factor (cf = M_{pDRdry}/M_{AMS}) was applied to M_{pDRwet} to obtain $M_{pDRwetc}$ ($M_{pDRwetc}= M_{pDRwet}$/cf).

The thermodynamic equilibrium model ISORROPIA II (Fountoukis et al., 2007) was used to estimate the ALW taken up by the inorganic aerosol compounds (hereafter "M_{ALWIOA}"), based on (1) the inorganic aerosol compound concentrations (NO_3^-, SO_4^{2-}, NH_4^+) measured by AMS with all other metal ions setting 0, and (2) the RH and temperature measured inside of pDR_{wet}. The calculated M_{ALWIOA} is then subtracted from M_{ALW} to obtain ALW caused by the organic aerosol compounds (hereafter "M_{ALWOA}", as shown in Eq.(2):

$$M_{ALWOA} = M_{ALW} - M_{ALWIOA} \quad (2)$$

Assuming an organic aerosol density of 1.4 g cm^{-3}, the κ_{OA} (units: 1) can be inferred from MALWOA following Eq.(3) (Nguyen et al., 2016):

$$\kappa_{OA} = M_{ALWOA} \div (\rho_w \times \frac{m_{OA}}{\rho_{OA}} \times \frac{RH}{1-RH}) \quad (3)$$

where RH is the relative humidity reported by pDR_{wet}, m_{OA} is the AMS measured organic aerosol mass concentration, ρ_{OA} is the organic aerosol density (1.4 g cm^{-3}), and ρw is the water density (1.0 g cm^{-3}). In this study, only the data with RH between [85% 95%] were considered for estimating κ_{OA} in order to (1) match the RH used in HTDMA, (2) reduce the uncertainty of aerosol mass concentration measured by pDR_{wet} under the RH over 95%, which is suggested by the pDR user manual, and also (3) ensure the inorganic aerosol is in an aqueous state. The derived κ_{OA} and ambient temperature and RH can be further used to estimate ambient ALW through the inverse calculations based on Eq.3 and Eq.2, and the information of ambient ALW can be very useful for the study of aqueous SOA formations/evolutions.

In this study, using AMS as the reference instrument for pDR_{dry} could introduce a certain level of uncertainty for the ALW estimation due to (1) the AMS's limited sensitivity to refractory aerosols (e.g. sea salt), and (2) the discrepancy size range detected by the pDR_{dry} and AMS. The coarse-mode particles (including the coarse-mode refractory aerosols) with diameter between 1 µm and 2.5 µm detected by pDR_{dry} will not be captured by the AMS. By simply assuming a constant mass ratio for the chemical composition of fine-mode and coarse-mode particles, the ratio of MALW associated with fine-mode particles to that associated with coarse-mode particles will correspond to the dry aerosol mass concentration of each mode. Consequently, the estimated MALW here based on the calibrated aerosol mass concentration from the pDRs using AMS as reference would only represent the liquid water in non-refractory PM_1. These factors collectively contribute to the uncertainty of the κ_{OA} calculation. Additionally, this uncertainty was further magnified when calculating MALWOA based on the estimate M_{ALWIOA} from ISORROPIA II. The absence of measurements for metal ions necessitated the assumption of "0" for all such ions in the ISORROPIA II inputs, further compounding the uncertainty, along with the inherent uncertainties of the ISORROPIA II model itself. Moreover, the uncertainty of calculating κ_{OA} will further come from using the empirical equation Eq.(3) and the assumed value for the density of organic compounds.

To approximate the uncertainty associated with this proposed method, we categorized the measured O:C ratio into bins with an increment of 0.05, ranging from 0.4 to 1.0, for each group with different aerosol source. We then assumed that the standard deviation of κ_{OA} within each bin reflects the uncertainty in the estimated κOA, based on the assumption κ_{OA} is linearly related to O:C ratio for each specific aerosol source group. The maximum standard deviation of κ_{OA} across all bins of the identified three groups was determined to be 0.08, which was expected as the upper limit of the uncertainty for κ_{OA}. More detailed information of the distribution of κ_{OA} in each bin for each group with different aerosol sources and its relationship with the measured O:C ratio is discussed in the following section "Variation of κ_{OA} with different aerosol sources". Meanwhile, it's crucial to acknowledge that this study does not account for the impact of black/brown carbon on the results, as both the pDR devices and the AMS do not detect black/brown carbon.

3 Results and discussion

3.1 Overview of measurements

The time series of all calibrated aerosol mass concentrations measured by the pDRs are shown in Fig. 2a, revealing significant discrepancies between pDR_{dryc} and pDR_{wetc} under high RH conditions (Fig. 2b). This highlights the contribution of ALW to the response of the pDR_{wetc}. As shown in Fig. 2b, the mass growth factor ($=M_{pDRwetc}/M_{pDRdryc}$) was around 2.5 (mainly between [24]) under the RH range [90% 100%], which was generally higher than the value (around 1.3) under the RH range [80% 90%]. Notably, there were several points with growth factors around 1.3under their RH range [90% 100%], suggesting their weaker hygroscopicity compared to the points with a growth factor between 2and 4. This discrepancy also implies different sources for these two distinct RH ranges.

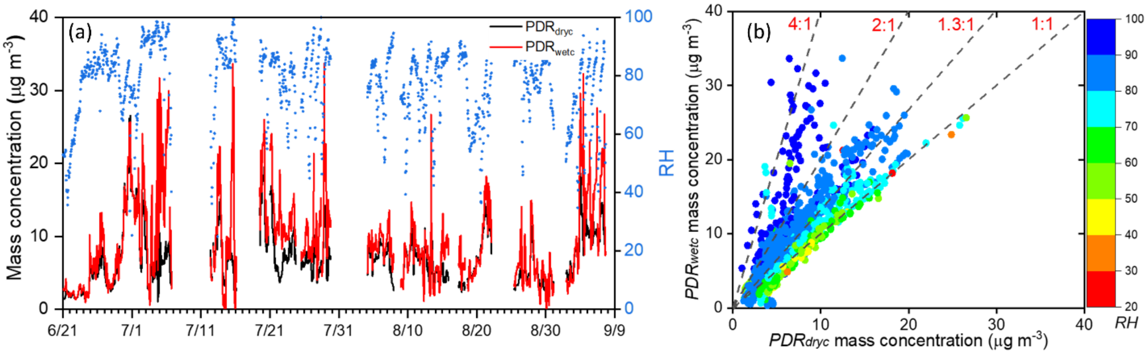

Figure 2. (a) The time series of 1-h average aerosol mass concentration measured by pDRwetc and pDR_{dryc}, and (b) the correlation scatter plot of pDRwetc and pDR_{dryc} colored by RH.

As described in the "METHODS" section, only the pDR_{wetc} with RH between [85% 95%] was considered for κ estimation, and the calculated M_{ALWIOA}, $M_{ALWOA,}$ and M_{ALW} (M_{ALW} =M_{ALWIOA}+ M_{ALWOA}) are shown in Fig. 3. ALW could be as high as about 18.6 μg m^{-3} with the related mass growth factor around 2.9. During the initial half of the deployment, there were some points with M_{ALWOA} below 0, and this occurred when M_{ALWIOA}, as estimated from the ISORROPIA II model, exceeded the total M_{ALW} derived from the two pDR measurements. Such negative values can be attributed to previously discussed uncertainties in either the calibration of the pDR devices or the estimations made by the ISORROPIA II model, and will also result negative κ_{OA}, as described below. When considering all the points with M_{ALWOA} over 0, ALW_{OA} showed significant contributions to the total wet aerosol mass concentration with an average fraction of 27% and a wide range of [15% 39%] for the [25%-75%]. This underscores the necessity of obtaining accurate κ_{OA} values to better obtain ALW_{OA} and evaluate its impact on aerosol evolution.

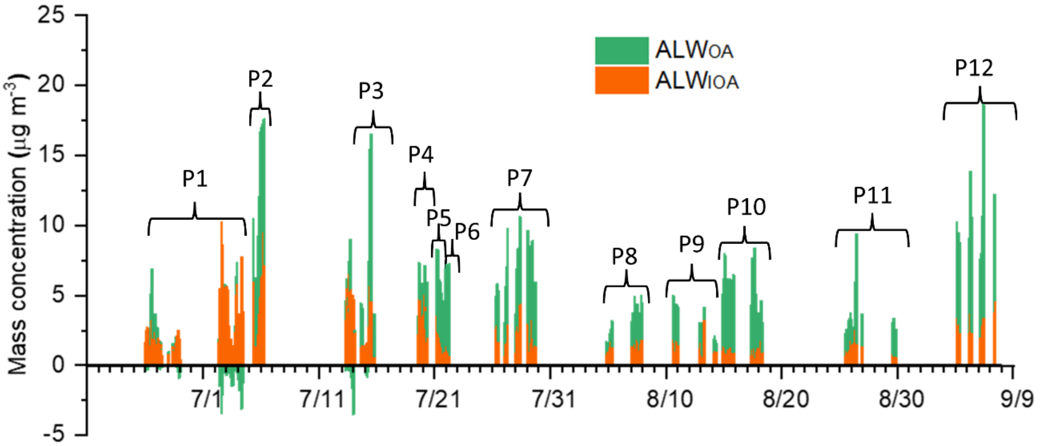

P1: 89 points on June 26, 27, 28, 29 and July 02, 03, 04
P2: 14 points on July 05, 06
P3: 33 points on July 13, 14, 15
P4: 17 points on July 19, 20
P5: 13 points on July 21
P6: 13 points on July 21, 22
P7: 41 points on July 26, 27, 28, 29
P8: 30 points on Aug. 04, 05, 07
P9: 28 points on Aug. 10, 11, 12, 13, 14
P10: 38 points on Aug. 14, 15, 17, 18
P11: 32 points on Aug. 25, 26, 29
P12: 21 points on Sep. 04, 05, 06,07

Figure 3. The time series of ALW_{OA} and ALW_{IOA} with a time resolution of 1-hr. (P1-P12 denote the different sub-periods mentioned in the following text with the data points and time periods of each subperiod indicated.)

3.2 Variation of κOA with different aerosol sources

The box and whiskers distribution of the derived κ_{OA} for each sub-period is shown in Fig. 4a, alongside the measured aerosol mass concentration in Fig. 4b. Sub-periods were categorized based on the back trajectories of each subperiod (Fig. S2-S7), and they were divided into three groups with different aerosol sources, including one group with aerosol having urban sources (marked in grey in Fig. 4, hereafter "Group1(urban)", Fig. S2 for their back trajectories), one group with aerosol having rural sources (marked in green in Fig. 4, hereafter "Group2(rural)", Fig. S3 for their back trajectories), and one group with aerosol affected by the wildfire plumes (marked in red in Fig. 4, hereafter "Group3(wildfire)",, Fig. S4-S7 for their back trajectories). Generally speaking, Group1(urban) showed relatively higher mass concentration and lower κ_{OA}, which agrees with findings from previous studies that the urban aerosol generally has a low hygroscopicity activity (Wu et al., 2016; Hong et al., 2018). At the same time, the points with κ_{OA} below 0 were predominantly found in P1 of Group1(urban) with values dipping to as low as -0.08, and these negative value fell within the expected upper limited uncertainty of κ_{OA} of 0.08 given the averaged κ_{OA} of P1 being around 0. The relatively low κ_{OA} in P1 followed their low O:C ratio, as shown in Fig. S8. Conversely, Group2(rural) exhibited higher values of κ_{OA} compared to other groups, which can be attributed to their exposure to long-term transport/reactions and consequently, a stronger hygroscopicity activity. Meanwhile, the data points of the subperiods (P10 and P11) of Group2(rural) were highly scattered, especially for plume back trajectories over the ocean, highlighting the uncertainty caused by the marine sea salt aerosol. The Group3(wildfire)demonstrated a big range of κ_{OA}, with the subperiod “P4” having the lowest κ_{OA} (an averaged value of 0.02, near to hydrophobic organics, Kuang et al., 2020; Han et al., 2022) and the highest mass concentration. Additionally, the subperiod “P4” exhibited the most notable transport pathway from western Canada to NYC metro regions (Fig. S4) compared to other wildfire plume cases (Fig. S5-S7). Considering all four of these cases of wildfire aerosol having an original wildfire source in western Canada, it is reasonable to infer the wildfire κ_{OA} could be strongly affected by the burning time of the original forests, the transport time from west to east, etc. (Garofalo et al., 2019), resulting in significant variation between different cases, warranting further investigation.

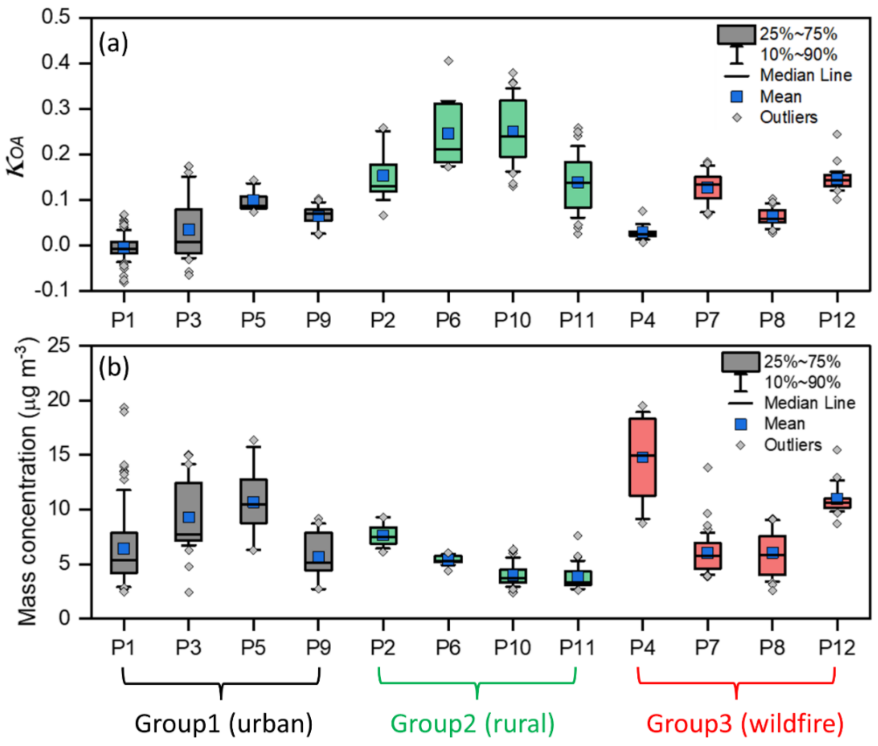

Figure 4. The box and whiskers distribution of κ$_{OA}$ and aerosol total mass concentration for each subperiod. (The time resolution of each data point is 1 hr. The subperiods being affected by urban plumes are marked in grey and categorized as Group1(urban), the ones being affected by rural environments are marked in green and categorized as Group2(rural), and the ones being affected by wildfire plumes are marked in red and categorized as Group3(wildfire)).

The derived subsaturated hygroscopicity of organic compounds in both Group1(urban) and the Group2(rural) exhibited a tight relationship with their O:C ratio, with the κ$_{OA}$ increasing as the O:C level rose while distinct slopes for each group, as shown in Fig. 5a and Fig. S8. The urban aerosol showed a much smaller linear slope (~0.24) between κ$_{OA}$ and O:C compared to the rural aerosol, which had a steeper linear slope of 0.50. The fitted linear slopes of this study closely resembled previous studies having similar organic aerosol sources. This supports previous findings that the hygroscopicity of urban organic aerosols is much less sensitive to variation in their oxidation level than rural organic aerosols (Wu et al., 2016; Hong et al., 2018). Fig. 5a also presents the derived slope from previous studies for various atmospheric conditions using more precise instruments for κ$_{OA}$, with the HTDMA for the urban aerosol in China by Hong et al. (2018) and the forest aerosols in Japan by Deng et al. (2019), the CCN counter (CCNc) for the rural mountain aerosols in USA by Zhang et al. (2019). The slope of 0.24 of Group1(urban) was near to the value reported in Guangzhou, China by Hong et al. (2018) and the slope of 0.50 aligned with findings from the forest/mountain aerosols (Deng et al., 2019; Zhang et al., 2019). The close alignment between the results of this study and those from previous research underscores the viability of this simpler system to offer reasonable estimates of κ$_{OA}$ in comparison to more precise and costly instruments, such as the HTDMA and the CCNc. It also shows the near-constant trends of κ$_{OA}$ for each period affected by the wildfire plumes, and that there were no clear linear relationships between κ$_{OA}$ and O:C for each period affected by the wildfire. This could be related to the complexity of the wildfire plumes and their long-term transport from west to east. More specially, they showed a negative relationship when combining all four wildfire periods (Fig. 5b), and further studies will need to verify this and investigate the possible reasons.

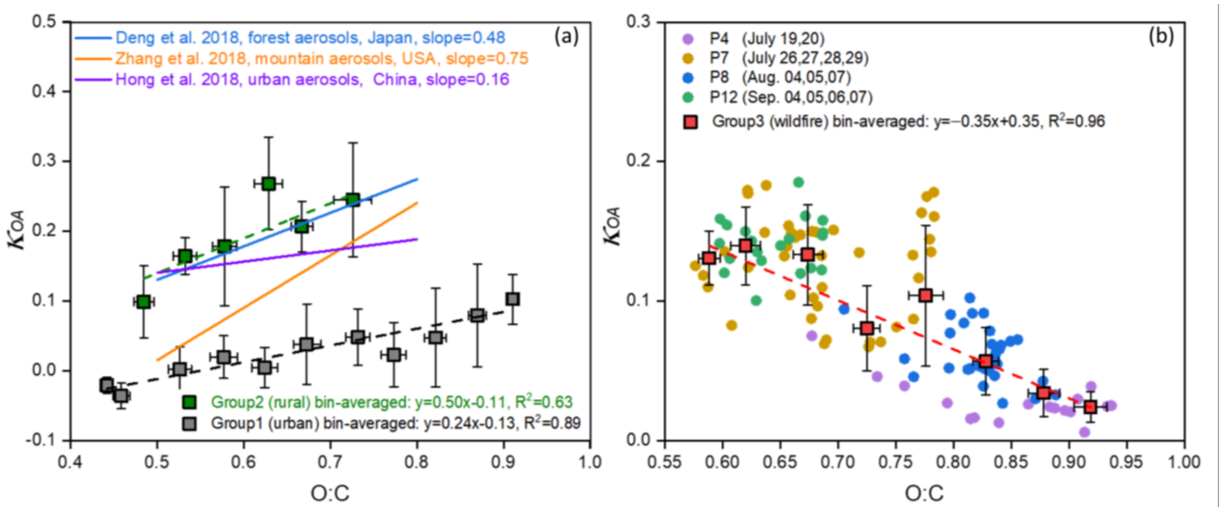

Figure 5. The relationship between κ$_{OA}$ and O:C of each group. (a) The relationship between κ$_{OA}$ and O:C for Group1(urban) (marked by grey) and Group2(rural) (marked by green). (Data points located in each O:C bin was

https://doi.org/10.5194/egusphere-2024-1390
Preprint. Discussion started: 11 July 2024

averaged to obtain the bin-averaged κ_{OA} and O:C, with the error bar showed their standard deviation in each bin. The bin-averaged κ_{OA} and O:C were fitted using the linear regression fit with the fitting line in dash. Meanwhile, the fitted slopes between κ_{OA} vs. O:C from previous studies were presented in solid lines, and were used to compare with the results of this study and to verify the feasibility of the proposed method). (b) The relationship between bin-averaged κ_{OA} and O:C for the aerosols affected by the wildfire transports (in red square with their standard deviation as error bar), and the relationship between κ_{OA} and O:C of each subperiod of Group3(wildfire) with a time resolution of 1-hr.

Once again, the distinctly different relationships between κ_{OA} and O:C between these three groups of organic aerosols indicate the substantial uncertainty in describing the hygroscopicity using a simplified average O:C ratio without considering the possible organic aerosol sources (Kuang et al., 2020; Han et al., 2022), and also highlights the necessity of deriving κ_{OA} based on direct measurements.

4 Conclusions

A simple optical scatter monitor system, containing two pDRs with one for dry aerosol and one for wet aerosol, was used to derive the organic aerosol hygroscopicity parameter (κ_{OA}) under subsaturated high humidity conditions (RH between [85% 95%]), after knowing the aerosol chemical compound mass concentrations. The derived κ_{OA} for the measurement period was largely dependent on the aerosol sources and showed different relationships with the organic aerosol oxidant level (i.e., O:C ratio in this study) for each classification of the aerosol source. κ_{OA} showed a positive linear relationship with O:C ratio for the urban aerosol and the rural aerosol with a much higher slope for the latter (0.24 urban vs. 0.50 rural). The fitted relationships agreed well with previous studies, supporting the feasibility of this simple system to estimate κ_{OA}. No clear relationship was shown for each period when the organic aerosol was influenced by the transported wildfire plumes. These different κ_{OA} vs. O:C relationships imply the necessity of estimation of κ_{OA} through direct measurements, rather than through a simple dependent relationship based on one kind of aerosol other properties (i.e., O:C ratio).

This approach offers a cost-effective alternative (given that two pDRs cost around $10,000) for estimating the κOA of ambient aerosols during field campaigns, especially when utilizing AMS or ACSM to measure the mass concentration of aerosol chemical compounds in situations where tools like HTDMA or CCNc are not available. Another possible more broadly application of this system could be to the US EPA Chemical Speciation Network (CSN) network for the period averaged κ_{OA} after knowing the time averaged mass concentration of each chemical compounds. The potential widespread use of this method is expected to enhance our understanding of κ_{OA} variations and their influence on CCN activities across various spatial and temporal scales. Moreover, it enables the calculation of ambient ALW from the derived κ_{OA}, taking into account ambient temperature and RH, which is particularly valuable for studies on atmospheric aqueous phases and the formation of secondary organic aerosols.

It should be noted that the measurements of aerosol liquid water (ALW) and the derived κ_{OA} in this study were not continuous due to our current inability of keeping the aerosol under a controlled high RH conditions for this current system, and this also limited the lab calibration/varication of this method using substances of known hygroscopic parameter. To resolve this issue, one possible update of this system could be adding a humidifier to the pDR for wet aerosol. This would make the system more similar to the widely used humidified nephelometer system, designed by NOAA for various DOE ARM Mobile Facilities (Burgos et al., 2019), and used by other research groups (Fierz-Schmidhauser et al., 2010; Kuang et al., 2020). Given that the pDR is a type of nephelometric monitor, it's logical to consider that other brands of nephelometric monitors might offer similar capabilities. The potential for broader applicability of this approach across different nephelometric monitoring devices is indeed promising and warrants validation through further research.

Data availability. The data set is available upon request from the corresponding author.

Author contributions. JZ preforms the calculation and data analysis; TZ and AC helped to the data collection; YL, MS, PL, AA, JS helped to interpret the results and revised the manuscript. JZ wrote the paper with contributions from all coauthors.

Competing interests. The author has declared that there are no competing interests.

Acknowledgements. This work has been supported through the New York State Energy Research and Development Authority (NYSERDA) Contract 183868. We acknowledge the support and assistance of NYS DEC personnel, Stony Brook University, and, in particular, the curator of the Flax Pond Marine Laboratory, Mr. Stephen Abrams.

References

Burgos, M. A., Andrews, E., Titos, G., Alados-Arboledas, L., Baltensperger, U., Day, D., Jefferson, A., Kalivitis, N., Mihalopoulos, N., Sherman, J., Sun, J., Weingartner, E., and Zieger, P.: A global view on the effect of water uptake on aerosol particle light scattering, Scientific Data, 6, 157, https://doi.org/10.1038/s41597-019-0158-7, 2019.

Cappa, C., Che, D., Kessler, S., Kroll, J., and Wilson, K.: Variations in organic aerosol optical and hygroscopic properties upon heterogeneous OH oxidation, J. Geophys. Res., 116, D15204, https://doi.org/10.1029/2011jd015918, 2011.

Cerully, K. M., Bougiatioti, A., Hite Jr., J. R., Guo, H., Xu, L., Ng, N. L., Weber, R., and Nenes, A.: On the link between hygroscopicity, volatility, and oxidation state of ambient and water-soluble aerosols in the southeastern United States, Atmos. Chem. Phys., 15, 8679–8694, https://doi.org/10.5194/acp-15-8679-2015, 2015.

Chang, R. Y.-W., Slowik, J. G., Shantz, N. C., Vlasenko, A., Liggio, J., Sjostedt, S. J., Leaitch, W. R., and Abbatt, J. P. D.: The hygroscopicity parameter (κ) of ambient organic aerosol at a field site subject to biogenic and anthropogenic influences: relationship to degree of aerosol oxidation, Atmos. Chem. Phys., 10, 5047–5064, https://doi.org/10.5194/acp-10-5047-2010, 2010.

Deng, Y., Yai, H., Fujinari, H., Kawana, K., Nakayama, T., and Mochida, M.: Diurnal variation and size dependence of the hygroscopicity of organic aerosol at a forest site in Wakayama, Japan: their relationship to CCN concentrations, Atmos. Chem. Phys., 19, 5889–5903, https://doi.org/10.5194/acp-19-5889-2019, 2019.

Ervens, B., Turpin, B. J., and Weber, R. J.: Secondary organic aerosol formation in cloud droplets and aqueous particles (aqSOA): a review of laboratory, field and model studies, Atmos. Chem. Phys., 11, 11069–11102, https://doi.org/10.5194/acp-11-11069-2011, 2011.

Fierz-Schmidhauser, R., Zieger, P., Wehrle, G., Jefferson, A., Ogren, J. A., Baltensperger, U., and Weingartner, E.: Measurement of relative humidity dependent light scattering of aerosols, Atmos. Meas. Tech., 3, 39–50, https://doi.org/10.5194/amt-3-39-2010, 2010.

Fountoukis, C. and Nenes, A.: ISORROPIA II: a computationally efficient thermodynamic equilibrium model for K^+–Ca^{2+}–Mg^{2+}–NH_4^+–Na^+–SO_4^{2-}–NO_3^-–Cl^-–H_2O aerosols, Atmos. Chem. Phys., 7, 4639–4659, https://doi.org/10.5194/acp-7-4639-2007, 2007.

Garofalo, L. A., Pothier, M. A., Levin, E. J. T., Campos, T., Kreidenweis, S. M., and Farmer, D. K.: Emission and Evolution of Submicron Organic Aerosol in Smoke from Wildfires in the Western United States, ACS Earth Space Chem., 3, 1237–1247, https://doi.org/10.1021/acsearthspacechem.9b00125, 2019.

Han, S., Hong, J., Luo, Q., Xu, H., Tan, H., Wang, Q., Tao, J., Zhou, Y., Peng, L., He, Y., Shi, J., Ma, N., Cheng, Y., and Su, H.: Hygroscopicity of organic compounds as a function of organic functionality, water solubility, molecular weight, and oxidation level, Atmos. Chem. Phys., 22, 3985–4004, https://doi.org/10.5194/acp-22-3985-2022, 2022.

Hong, J., Xu, H., Tan, H., Yin, C., Hao, L., Li, F., Cai, M., Deng, X., Wang, N., Su, H., Cheng, Y., Wang, L., Petäjä, T., and Kerminen, V.-M.: Mixing state and particle hygroscopicity of organic-dominated aerosols over the Pearl River Delta region in China, Atmos. Chem. Phys., 18, 14079–14094, https://doi.org/10.5194/acp-18-14079-2018, 2018.

Jimenez, J. L., Canagaratna, M. R., Donahue, N. M., Prevot, A. S. H., Zhang, Q., Kroll, J. H., DeCarlo, P. F., Allan, J. D., Coe, H., Ng, N. L., Aiken, A. C., Docherty, K. S., Ulbrich, I. M., Grieshop, A. P., Robinson, A. L., Duplissy, J., Smith, J. D., Wilson, K. R., Lanz, V. A., Hueglin, C., Sun, Y. L., Tian, J., Laaksonen, A., Raatikainen, T., Rautiainen, J., Vaattovaara, P., Ehn, M., Kulmala, M., Tomlinson, J. M., Collins, D. R., Cubison, M. J., Dunlea, E. J., Huffman, J. A., Onasch, T. B., Alfarra, M. R., Williams, P. I., Bower, K., Kondo, Y., Schneider, J., Drewnick, F., Borrmann, S., Weimer, S., Demerjian, K., Salcedo, D., Cottrell, L., Griffin, R., Takami, A., Miyoshi, T., Hatakeyama, S., Shimono, A., Sun, J. Y., Zhang, Y. M., Dzepina, K., Kimmel, J. R., Sueper, D., Jayne, J. T., Herndon, S. C., Trimborn, A. M., Williams, L. R., Wood, E. C., Middlebrook, A. M., Kolb, C. E., Baltensperger, U., and Worsnop, D. R.: Evolution of Organic Aerosols in the Atmosphere, Science, 326, 1525-1529, https://doi.org/10.1126/science.1180353, 2009.

Kuang, Y., Xu, W., Tao, J., Ma, N., Zhao, C., and Shao, M.: A Review on Laboratory Studies and Field Measurements of Atmospheric Organic Aerosol Hygroscopicity and Its Parameterization Based on Oxidation Levels, Curr. Pollut. Rep., 6, 410–424, https://doi.org/10.1007/s40726-020-00164-2, 2020.

Kuang, Y., He, Y., Xu, W., Zhao, P., Cheng, Y., Zhao, G., Tao, J., Ma, N., Su, H., Zhang, Y., Sun, J., Cheng, P., Yang, W., Zhang, S., Wu, C., Sun, Y., and Zhao, C.: Distinct diurnal variation in organic aerosol hygroscopicity and its relationship with oxygenated organic aerosol, Atmos. Chem. Phys., 20, 865–880, https://doi.org/10.5194/acp-20-865-2020, 2020.

Kuwata, M., Shao, W., Lebouteiller, R., and Martin, S. T.: Classifying organic materials by oxygen-to-carbon elemental ratio to predict the activation regime of Cloud Condensation Nuclei (CCN), Atmos. Chem. Phys., 13, 5309–5324, https://doi.org/10.5194/acp-13-5309-2013, 2013.

Liu, P., Song, M., Zhao, T., Gunthe, S.S., Ham, S., He, Y., Qin, Y.M., Gong, Z., Amorim, J.C., Bertram, A.K. and Martin, S.T.: Resolving the mechanisms of hygroscopic growth and cloud condensation nuclei activity for organic particulate matter. Nature communications, 9(1), p.4076, https://doi.org/10.1038/s41467-018-06622-2, 2018.

Lance, S., Raatikainen, T., Onasch, T. B., Worsnop, D. R., Yu, X.-Y., Alexander, M. L., Stolzenburg, M. R., McMurry, P. H., Smith, J. N., and Nenes, A.: Aerosol mixing state, hygroscopic growth and cloud activation efficiency during MIRAGE 2006, Atmos. Chem. Phys., 13, 5049–5062, https://doi.org/10.5194/acp-13-5049-2013, 2013.

Lambe, A. T., Onasch, T. B., Massoli, P., Croasdale, D. R., Wright, J. P., Ahern, A. T., Williams, L. R., Worsnop, D. R., Brune, W. H., and Davidovits, P.: Laboratory studies of the chemical composition and cloud condensation nuclei (CCN) activity of secondary organic aerosol (SOA) and oxidized primary organic aerosol (OPOA), Atmos. Chem. Phys., 11, 8913–8928, https://doi.org/10.5194/acp-11-8913-2011, 2011.

Massoli, P., Lambe, A. T., Ahern, A. T., Williams, L. R., Ehn, M., Mikkilä, J., Canagaratna, M. R., Brune, W. H., Onasch, T. B., Jayne, J. T., Petäjä, T., Kulmala, M., Laaksonen, A., Kolb, C. E., Davidovits, P., and Worsnop, D. R.: Relationship between aerosol oxidation level and hygroscopic properties of laboratory generated secondary organic aerosol (SOA) particles, Geophys. Res. Lett., 37, L24801, https://doi.org/10.1029/2010gl045258, 2010.

Ng, N. L., Herndon, S. C., Trimborn, A., Canagaratna, M. R., Croteau, P. L., Onasch, T. B., Sueper, D., Worsnop, D. R., Zhang, Q., Sun, Y. L., and Jayne, J. T.: An Aerosol Chemical Speciation Monitor (ACSM) for Routine Monitoring of the Composition and Mass Concentrations of Ambient Aerosol, Aerosol Sci. Tech., 45, 780–794, https://doi.org/10.1080/02786826.2011.560211, 2011.

Nguyen, T. K. V., Zhang, Q., Jimenez, J. L., Pike, M., and Carlton, A. G.: Liquid water: ubiquitous contributor to aerosol mass, Environ. Sci. Tech. Let., 3, 257–263, https://doi.org/10.1021/acs.estlett.6b00167, 2016.

Petters, M. D. and Kreidenweis, S. M.: A single parameter representation of hygroscopic growth and cloud condensation nucleus activity, Atmos. Chem. Phys., 7, 1961–1971, https://doi.org/10.5194/acp-7-1961-2007, 2007.

Pöhlker, M.L., Pöhlker, C., Quaas, J., Mülmenstädt, J., Pozzer, A., Andreae, M.O., Artaxo, P., Block, K., Coe, H., Ervens, B. and Gallimore, P.: Global organic and inorganic aerosol hygroscopicity and its effect on radiative forcing. Nature communications, 14(1), p.6139. https://doi.org/10.1038/s41467-023-41695-8, 2023.

Rickards, A. M. J., Miles, R. E. H., Davies, J. F., Marshall, F. H., and Reid, J. P.: Measurements of the sensitivity of aerosol hygroscopicity and the κ parameter to the O/C ratio, J. Phys. Chem. A, 117, 14120–14131, https://doi.org/10.1021/jp407991n, 2013.

Seinfeld, J.H. and Pandis, S.N.: Atmospheric chemistry and physics: from air pollution to climate change. John Wiley & Sons, 2016

Shrivastava, M., Cappa, C. D., Fan, J., Goldstein, A. H., Guenther, A. B., Jimenez, J. L., Kuang, C., Laskin, A., Martin, S. T., Ng, N. L., Petaja, T., Pierce, J. R., Rasch, P. J., Roldin, P., Seinfeld, J. H., Shilling, J., Smith, J. N., Thornton, J. A., Volkamer, R., Wang, J., Worsnop, D. R., Zaveri, R. A., Zelenyuk, A., and Zhang, Q.: Recent advances in understanding secondary organic aerosol: implications for global climate forcing, Rev. Geophys., 55, 509–559, https://doi.org/10.1002/2016RG000540, 2017.

Wang, Y., Voliotis, A., Hu, D., Shao, Y., Du, M., Chen, Y., Kleinheins, J., Marcolli, C., Alfarra, M. R., and McFiggans, G.: On the evolution of sub- and super-saturated water uptake of secondary organic aerosol in chamber experiments from mixed precursors, Atmos. Chem. Phys., 22, 4149–4166, https://doi.org/10.5194/acp-22-4149-2022, 2022.

Wu, Z. J., Poulain, L., Henning, S., Dieckmann, K., Birmili, W., Merkel, M., van Pinxteren, D., Spindler, G., Müller, K., Stratmann, F., Herrmann, H., and Wiedensohler, A.: Relating particle hygroscopicity and CCN activity to chemical composition during the HCCT-2010 field campaign, Atmos. Chem. Phys., 13, 7983–7996, https://doi.org/10.5194/acp-13-7983-2013, 2013.

Wu, Z. J., Zheng, J., Shang, D. J., Du, Z. F., Wu, Y. S., Zeng, L. M., Wiedensohler, A., and Hu, M.: Particle hygroscopicity and its link to chemical composition in the urban atmosphere of Beijing, China, during summertime, Atmos. Chem. Phys., 16, 1123–1138, https://doi.org/10.5194/acp-16-1123-2016, 2016.

Zhang, J., Marto, J. P., and Schwab, J. J.: Exploring the applicability and limitations of selected optical scattering instruments for PM mass measurement, Atmos. Meas. Tech., 11, 2995–3005, https://doi.org/10.5194/amt-11-2995-2018, 2018.

Zhang, J., Lance, S., Wang, X., Wang, J. and Schwab, J.J.: Estimation of aerosol liquid water from optical scattering instruments using ambient and dried sample streams. Atmos. Environ, 239, 117787, https://doi.org/10.1016/j.atmosenv.2020.117787, 2020

Zhang, J., Ninneman, M., Joseph, E., Schwab, M. J., Shrestha, B., and Schwab, J. J.: Mobile Laboratory Measurements of High Surface Ozone Levels and Spatial Heterogeneity During LISTOS 2018: Evidence for Sea Breeze Influence, J. Geophys. Res.-Atmos., 125, 1–12, https://doi.org/10.1029/2019JD031961, 2020.

Zhang, J., Lance, S., Brandt, R., Marto, J., Ninneman, M. and Schwab, J.: Observed below-cloud and cloud interstitial submicron aerosol chemical and physical properties at Whiteface Mountain, New York, during August 2017. ACS Earth and Space Chem., 3(8), pp.1438-1450, https://doi.org/10.1021/acsearthspacechem.9b00117, 2019

Zhang, Q., Jimenez, J., Canagaratna, M., Allan, J., Coe, H., Ulbrich, I., Alfarra, M., Takami, A., Middlebrook, A., Sun, Y., Dzepina, K., Dunlea, E., Docherty, K., De Carlo, P., Salcedo, D., Onasch, T., Jayne, J., Miyoshi, T., Shimono, A., Hatakeyama, S., Takegawa, N., Kondo, Y., Schneider, J., Drewnick, F., Borrmann, S., Weimer, S., Demerjian, K., Williams, P., Bower, K., Bahreini, R., Cottrell, L., Griffin, R., Rautiainen, J., Sun, J., Zhang, Y., and Worsnop, D.: Ubiquity and dominance of oxygenated species in organic aerosols in anthropogenically-influenced Northern Hemisphere midlatitudes, Geophys. Res. Lett., 34, L13801, https://doi.org/10.1029/2007GL029979, 2007.